ORGANOMETALLICS

Article

Cite This: *Organometallics* XXXX, XXX, XXX–XXX

pubs.acs.org/Organometallics

Comprehensive Study of the Reactions Between Chelating Phosphines and Ni(cod)$_2$

Andrew L. Clevenger,[†] Ryan M. Stolley,[†] Nicholas D. Staudaher,[†] Noman Al,[†] Arnold L. Rheingold,[‡] Ryan T. Vanderlinden,[†] and Janis Louie*[,†]

[†]Department of Chemistry, The University of Utah, 315 South 1400 East, Room 2020, Salt Lake City, Utah 84112, United States

[‡]Department of Chemistry and Biochemistry, University of California, San Diego, 9500 Gilman Drive, La Jolla, California 92093, United States

Supporting Information

ABSTRACT: A comprehensive study of the reactions of chelating phosphines with Ni(cod)$_2$ to form (phosphine)Ni(cod), (phosphine)$_2$Ni, or mixtures thereof is presented. A series of (phosphine)Ni(cod) complexes were isolated and characterized. The structural differences between the (phosphine)Ni(cod) and (phosphine)$_2$Ni complexes were examined using X-ray crystallography and ^{1}H and ^{31}P NMR spectroscopy. In addition, the effects of ring size, rigidity, and bulk of the phosphine backbone on the formation of either (phosphine)Ni(cod) or (phosphine)$_2$Ni were investigated. These studies show that the Ni−P bond lengths in both the (phosphine)-Ni(cod) and (phosphine)$_2$Ni complexes and the size of the ring formed by the chelating phosphine and Ni are crucial in determining whether or not (phosphine)Ni(cod) complexes can be isolated. Other factors such as π-stacking interactions were found to have marginal influence.

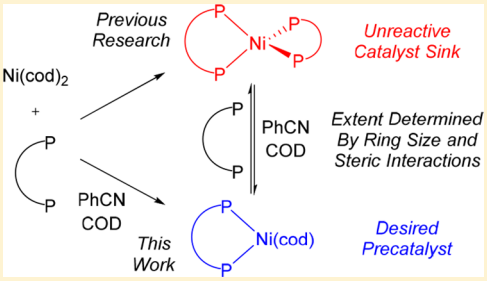

INTRODUCTION

Transition metal catalyzed reactions are predominated by use of second- or third-row transition metals as catalysts. Of the late transition metals, the prevalence of palladium has seen exponential growth, primarily in cross-coupling reactions. This is owing to the fact that palladium is very efficient at performing the two-electron transformations required for most organic reactions.[1] However, palladium-catalyzed cross coupling reactions have limitations, such as a propensity for β-H elimination.[2] In addition, oxidative addition reactions at palladium are more sluggish when using electrophilic substrates.[3] As a result, new catalytic cross-coupling reactions of two electrophilic substrates using nickel catalysts have been on the rise in recent years,[4] mirroring a similar path of palladium. Nickel is intriguing due to its ability to access a wide range of oxidation states from 0 to +4, which allows for both single-electron and two electron reactivity. Single electron reactivity can mitigate problems with β-H elimination and provide for more facile transmetalation, which is a critical step in cross-coupling chemistry.[2] Ligands used in nickel catalysis mirror those used in palladium catalysis. In particular, monodentate phosphines are very popular and widely utilized. Not surprisingly, the electronic and steric requirements for the phosphine when ligated to nickel are subtly but noticeably different than when bound to palladium, and those needs are just beginning to be understood.[5]

Chelating phosphines have had less success than monodentate phosphines when utilized in nickel catalysis.[6] The scarcity of catalytic reactions involving chelating phosphines is somewhat surprising considering the different reactivity relative to monodentate phosphines that chelating phosphines impart. For example, nickel intermediates with chelating phosphines are less likely to undergo β-H elimination side reactions.[7] These intermediates are also crucial for effective stereo- and regiocontrol of products.[4b,8] Two general methods exist for utilizing chelating phosphines in nickel(0) catalysis. One uses the *in situ* reduction of a (phosphine)Ni(II)X$_2$ species (X = Cl, Br) to form the active Ni(0) catalyst. The other involves the *in situ* formation of the precatalyst through the combination of Ni(cod)$_2$ and a phosphine ligand. This precatalyst is generally (phosphine)Ni(cod). The formation of this complex is followed by the displacement of COD by the desired substrate in the reaction. This research focuses on the second of these methods, which has the advantage of avoiding reducing conditions and having a Ni source readily available. While catalytic reactions exist that use Ni(II) under oxidative conditions, these reactions are not as common as those that use oxidation states between Ni(0) and Ni(II).

Although systematic variation of Ni(cod)$_2$/phosphine ratios are commonly examined, knowledge of the actual nickel precatalyst that forms in solution is often absent and the secondary ligand effects on these reactions are regularly negated or underexplored. As a result, the cause of an unsuccessful reaction may be the incompatible stereoelectronic properties of the phosphine *or* the formation of an unreactive

Received: June 27, 2018

DOI: 10.1021/acs.organomet.8b00438
Organometallics XXXX, XXX, XXX–XXX

catalyst sink, such as a saturated Ni phosphine complex, among myriad other problems. Thus, chelating phosphines may be underutilized, despite their potential to greatly expand the scope of nickel-based catalytic chemistry, because of their propensity to form undesired $(phosphine)_2Ni$.[9]

One chelating phosphine that has successfully been used in a catalytic system with $Ni(cod)_2$ is 1,1-bis(diphenylphosphino)-ferrocene (DPPF). When reacted in a 1:1 ratio with $Ni(cod)_2$, DPPF only forms (dppf)Ni(cod) with no $(dppf)_2Ni$ observed.[9a,b,10] This unique reactivity has been exploited in both catalytic and stoichiometric reactions. For example, Schoenebeck and co-workers reported a successful nickel-catalyzed trifluoromethylthiolation using a $Ni(cod)_2$/DPPF system. However, when 1,2-bis(diphenylphosphino)ethane (DPPE) was employed as a ligand in this reaction, the formation of $(dppe)_2Ni$ doubled the energy barrier of the key oxidative addition step.[9a,b] This barrier was doubled due to the need to dissociate one of the DPPE ligands from $(dppe)_2Ni$ in order to facilitate oxidative addition. The amount of active catalyst was also reduced by the formation of $(dppe)_2Ni$. The formation of this unwanted catalyst sink prevented evaluation of the effectiveness of DPPE in nickel-catalyzed trifluoromethylthiolation and narrowed the ligand scope of the reaction.

In terms of stoichiometric transformations, our group recently published syntheses and full characterizations of a library of (dppf)Ni(ketene) complexes. A screen of chelating phosphines showed that most formed $(phosphine)_2Ni$ when reacted with $Ni(cod)_2$ regardless of the presence or absence of ketene. This problem was further exacerbated by the fact that formation of $(phosphine)_2Ni$ is concomitant with the existence of unreacted $Ni(cod)_2$, which promoted unwanted side reactions with the starting materials.[10]

In a prior report, we showed that the combination of the chelating phosphine Xantphos[9e] and $Ni(cod)_2$ leads to the precipitation of insoluble $(Xantphos)_2Ni$. However, addition of benzonitrile and a π-substrate (eq 1) resulted in the formation of a variety of (Xantphos)Ni(π-L) complexes **1**–**5** (Figure 1).[11] The proposed mechanism (Scheme 1) involves

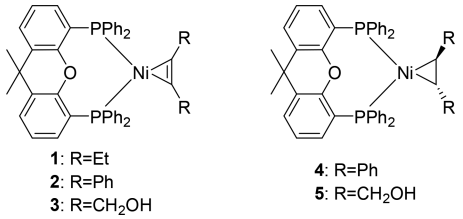

Figure 1. Synthesized (Xantphos)Ni(π-L) complexes **1**–**5**

replacement of an arm of the chelating phosphine by the nitrile binding through the lone pair on the terminal nitrogen, followed by a hapticity shift to η^2-NC that is concurrent with dissociation of one ligand. This process and its reverse reaction allows for equilibrium between $(Xantphos)_2Ni$ and (Xantphos)Ni(η^2-NC(Ph)). In order to form (Xantphos)Ni(π-L), benzonitrile is replaced by a stronger binding π substrate in solution where the strength of the nickel-π interaction drives the equilibrium forward. Importantly, a reaction of Xantphos, $Ni(cod)_2$, and π-substrate gave only $(Xantphos)_2Ni$ with no (Xantphos)Ni(π-L) observed, demonstrating the need for benzonitrile to bind to Ni and start the process of removing a phosphine from $(Xantphos)_2Ni$. The discovery that benzonitrile traps ligand dissociation of a

Scheme 1. Formation of (Xantphos)Ni(3-hexyne) through Use of Benzonitrile to Displace one Xantphos Ligand from $(Xantphos)_2Ni$

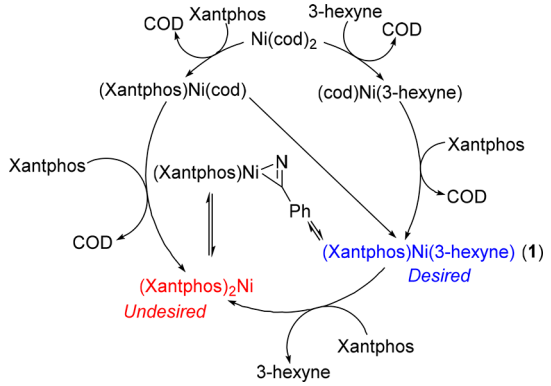

chelating phosphine and promotes the conversion of catalytically inactive $(Xantphos)_2Ni$ into the catalytically active species (Xantphos)Ni(π-L) was, to our knowledge, the first of its kind and provides a launching pad for the discovery of new Ni-catalyzed reactions utilizing chelating phosphines. This phenomenon has also been observed by Hartwig and co-workers using BINAP and $Ni(cod)_2$ for a Ni-catalyzed arylation of ketones. Addition of benzonitrile to the mixture of phosphine and $Ni(cod)_2$ was essential to the formation of the active catalyst.[6f,h]

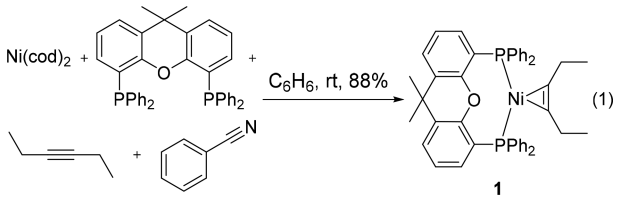

Herein, we report our investigations into the general use of nitrile to promote the formation of a family of (phosphine)-Ni(cod) complexes, which may serve as more active precatalysts and allow for the expanded use of these potentially powerful class of compounds. In order to quantify the usefulness of this method, the effect of the addition of nitrile on the ratio of (phosphine)Ni(cod)/$(phosphine)_2Ni$ complexes in a reaction was investigated. These results give greater insight into the formation of the precatalysts in nickel-catalyzed reactions.

RESULTS

The ligands in this study (Table 1, columns 1 and 2) were chosen in order to perform a systematic survey of the effects of changing the size and rigidity of the phosphine backbone on the equilibrium between the heteroleptic (phosphine)Ni(cod) complex and the homoleptic $(phosphine)_2Ni$ complex. These studies started by using bidentate chelating phosphines with aliphatic backbones. The backbone size ranged from one carbon (DPPM) to five carbons (DPPPentane). Complementary ligands such as DPPMB and DPPBenz allowed comparison of backbone rigidity, as these phosphines have phenyl rings in their backbones. DPEPhos and Xantphos vary by the added rigidity of the xanthene backbone in Xantphos. As previously stated, other research has shown that DPPF only forms (dppf)Ni(cod) when mixed with $Ni(cod)_2$ in a 1:1 ratio.[9a,b,10]

DOI: 10.1021/acs.organomet.8b00438
Organometallics XXXX, XXX, XXX–XXX

Table 1. Chelating Phosphine Ligands Studied for This Work[a]

Column Number	1	2	3	4	5	6	7	8	9
Entry	Ligand	Structure	1:1 P:Ni	15% PhCN	1.3 eq PhCN	4 eq PhCN	2 eq COD	10 eq COD	20 eq COD
1	DPPE		1:2	1:2	1:1	1:2	1:3	1:4	1:2
2	DPPP		1:10	1:10	1:10	1:10	1:6	1:12	1:2
3	(*p*-F)DPPB	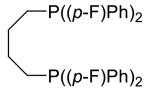	10:1	1:0	1:0	2:1	20:1	1:0	1:0
4	DPPB		15:1	1:0	1:0	1:1	1:3	1:0	1:0
5	(*p*-OMe)DPPB	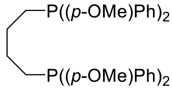	1:0	1:0	1:0	3:2	2:1	1:0	1:0
6	DPPPentane	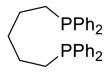	2:3	5:4	2:3:2[a]	1:3 +linear oligomers	2:3	5:4	1:1
7	DPPBenz	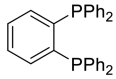	8:1	3:1	3:1	1:1	2:1	4:3	3:1
8	DPPMB	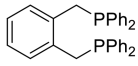	1:6	4:5	8:10:1[a]	2:0:1[a]	2:1	2:5	6:1
9	BIPHEP	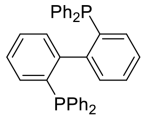	3:1	1:2	2:3:1[a]	1:1 +linear oligomers	2:3	1:1	1:5
10	BINAP	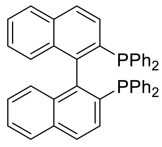	2:1	20:7:1[a]	4:1:2[a]	1:0:1[a]	6:3:1[a]	1:0	1:0
11	Xantphos	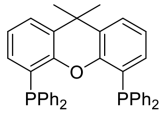	1:8	0:1	0:1	0:1	0:1	1:10	0:1
12	DPEPhos	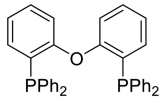	n/a	n/a	n/a	n/a	n/a	n/a	n/a
13	DPPF	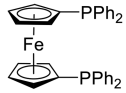	n/a	n/a	n/a	n/a	n/a	n/a	n/a

[a]Ratios of (phosphine)Ni(cod)/(phosphine)$_2$Ni when the phosphine and Ni(cod)$_2$ are mixed in a 1:1 ratio with no additives, of same experiment with differing amounts of benzonitrile, and of same experiment with 1.3 equiv of nitrile and differing amounts of COD. [b]Ratio is (phosphine)Ni(cod)/(phosphine)$_2$Ni/(phosphine)Ni(η^2-NC(Ph)).

Initial mixture of the chelating phosphine ligands in a 1:1 ratio with Ni(cod)$_2$ confirmed and extended the findings of our group and others, namely, that each ligand besides DPPF and DPEPhos formed (phosphine)$_2$Ni along with (phosphine)Ni(cod) (Scheme 2a) in various molar equivalencies (Table 1, column 3, entries 1−13).

Previously, the addition of nitrile in the presence of a π-substrate was sufficient to remove one Xantphos ligand from (Xantphos)$_2$Ni and form (Xantphos)Ni(π-L) complexes as the final product of the ligand substitution. However, the potential of nitrile to begin the process of the removing a phosphine from other (phosphine)$_2$Ni complexes in the presence of COD

DOI: 10.1021/acs.organomet.8b00438
Organometallics XXXX, XXX, XXX−XXX

Scheme 2. Experiments for Which the Results Are Shown in Table 1[a]

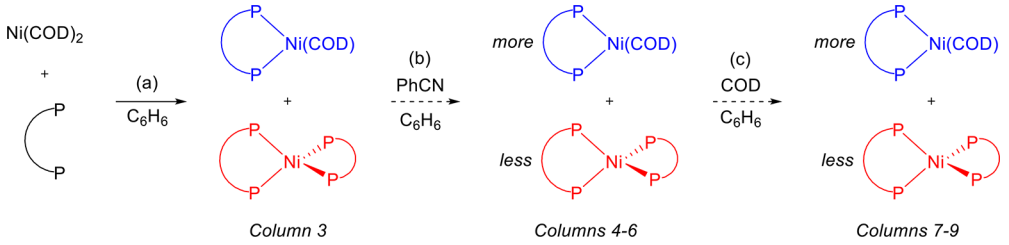

[a](a) Mixture of 1 equiv of Ni(cod)$_2$ and 1 equiv of a chelating phosphine. (b) Addition of benzonitrile. (c) Addition of excess COD.

to form (phosphine)Ni(cod) has not been investigated. To gather information about this effect, differing amounts of benzonitrile were added to mixtures of 1:1 Ni(cod)$_2$/phosphine. The addition of 0.15, 1.3, and 4 equiv of benzonitrile to these mixtures (Scheme 2b; Table 1, columns 4−6, entries 1−13) was generally not effective forming more (phosphine)Ni(cod). The cases where the addition of nitrile had the largest effect were with DPPMB (entry 8) and BINAP (entry 9), but a substantial amount of (phosphine)Ni(η^2-NC(Ph)) complex was observed along with the desired (phosphine)Ni(cod) complex. These results showed that addition of more benzonitrile was not sufficient to isolate (phosphine)Ni(cod) complexes without the addition of more COD.

The ratios from the reaction of 1 equiv of Ni(cod)$_2$, 1 equiv of phosphine, 1.3 equiv of benzonitrile, and either 2, 10, or 20 equiv of COD (Scheme 2c; Table 1, columns 7−9, entries 1−13) allow for a few conclusions to be drawn. If the (phosphine)$_2$Ni complex is susceptible to benzonitrile binding to facilitate ligand removal (e.g., DPPB (entries 3−5), DPPMB (entry 8), and BINAP (entry 10)) then the addition of more COD helps to favor the (phosphine)Ni(cod) complex. If the (phosphine)$_2$Ni complex is not very susceptible to benzonitrile (e.g DPPE (entry 1), DPPP (entry 2)), then the addition of COD does not have a large effect on the ratio of (phosphine)Ni(cod)/(phosphine)$_2$Ni.

While it was difficult to determine trends in much of these data, one aspect that stood out was that the three phosphines that gave the most promising results (DPPB, DPPMB, and BINAP) also were ligands that form seven-membered rings with Ni. The respective (phosphine)$_2$Ni complexes of these phosphines were the most likely to be susceptible to removal of a phosphine using benzonitrile, and DPPB formed about 20 times more (dppb)Ni(cod) than (dppb)$_2$Ni in most of the experiments (Table 1, entry 4). As a result, these phosphines were found to be the most suitable for a synthesis and isolation of their respective (phosphine)Ni(cod) complexes. (DPEPhos)Ni(cod) (**6**) was isolated in an 85% yield by simply mixing 1 equiv of DPEPhos and Ni(cod)$_2$. Isolation of other (phosphine)Ni(cod) complexes required the addition of nitrile and COD, as shown by the NMR scale experiments in Table 1. Isolations of (dppb)Ni(cod) (**7**) (95% yield), (dppmb)Ni(cod) (**8**) (89% yield), and (*rac*-binap)Ni(cod) (**9**) (65% yield) were carried out by using the reaction conditions shown in Table 2 (eq 2). The solvent was switched to THF for the reactions to form **8** and **9** to assist the solubility of the starting materials. None of these reactions required more than 1.3 equiv of benzonitrile. The synthesis of complex **7** needed 10 equiv of COD to push the reaction to completion, while the synthesis of **8** needed 20 equiv of COD. Complex **9** required 65 equiv of COD and 4 days of stirring in THF before it could be isolated.

Table 2. Reaction Conditions for the Synthesis of (Phosphine)Ni(cod) Complexes[a]

entry	phosphine	COD (equiv)	days	yield
1	DPEPhos (B)	0	1	85% (**6**)
2	DPPB (B)	10	1	95% (**7**)
3	DPPMB (T)	65	4	89% (**8**)
4	*rac*-BINAP (T)	20	1	65% (**9**)

[a]All reactions used 1.3 equiv of benzonitrile. B = benzene as solvent. T = THF as solvent.

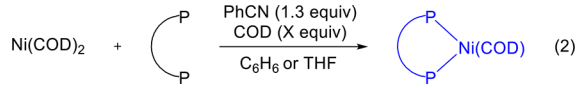

Derivatives of DPPB (1,4-bis(bis(4-fluorophenyl)-phosphino)butane ((*p*-F)DPPB), Table 1, column 2, entry 3 and 1,4-bis(bis(4-methoxyphenyl)phosphino)butane ((*p*-OMe)DPPB), Table 1, column 2, entry 5) were synthesized in order to examine the effects of changing the electronic properties of the ligand. Significant changes were not observed with added *p*-OMe and *p*-F groups to the substituents of the phosphines of DPPB (Table 1, entries 3−5).

Benzonitrile was used for all of the initial studies due to its previous use in the syntheses of (Xantphos)Ni(π-L) complexes.[11] For completeness, other nitriles, varying in both their steric and electronic properties, were screened. The ratios between (phosphine)Ni(cod) and (phosphine)$_2$Ni were examined when DPPE, DPPP, and DPPMB were reacted under the same conditions as those in Table 1, but with electronically and sterically modified nitriles replacing benzonitrile (eq 3). The phosphines were chosen in order to inspect a range of reactivity of the (phosphine)$_2$Ni complexes with nitrile. Previous studies showed that (dppe)$_2$Ni and (dppp)$_2$Ni were not reactive with benzonitrile (Table 1, entries 1 and 2), while (dppmb)$_2$Ni was reactive and (dppmb)Ni-(COD) was isolated (Table 1, entry 8; Table 2, entry 3). These results are shown in Table 3. As with the previous experiments involving COD, if the (phosphine)$_2$Ni complex was not susceptible to removal of one ligand by benzonitrile, then the change of either the electronics or sterics of the nitrile did not have a significant effect on the ratio. Both (dppe)$_2$Ni and (dppp)$_2$Ni were not reactive with benzonitrile and changing the nitrile did not result in an appreciable change in the ratio of (phosphine)Ni(cod)/(phosphine)$_2$Ni. With DPPMB, a more electron donating nitrile (4-methoxybenzonitrile, Table 3, entry 2) slightly increased the amount of (dppmb)Ni (cod) as compared to the reaction with just benzonitrile (Table 3, entry 1). When the electron deficient

DOI: 10.1021/acs.organomet.8b00438
Organometallics XXXX, XXX, XXX−XXX

Table 3. Results from Experiments with Different Nitriles

Entry	Nitrile	DPPE	DPPP	DPPMB
1	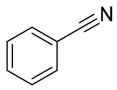	3:4	1:10	5:6
2	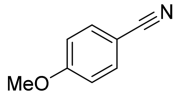	1:1	1:70	1:2
3	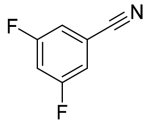	2:3	1:20	5:2:10[a]
4		1:1	1:50	5:7
5		10:9	n/a	5:6
6		10:9	1:60	1:1

[a]Ratio is (phosphine)Ni(cod)/(phosphine)$_2$Ni/(phosphine)Ni(η^2-NC(Ar)).

3,5-difluorobenzonitrile was tested, a significant amount of (dppmb)Ni(η^2-NC((3,5-F)Ph)) formed alongside (dppmb)-Ni(cod) and (dppmb)$_2$Ni (Table 3, entry 3). Alkyl nitriles such as ethylnitrile (Table 3, entry 4), isopropylnitrile (Table 3, entry 5), and *tert*-butylnitrile (Table 3, entry 6) did not have a significant effect on the ratios of (dppmb)Ni(cod)/(dppmb)$_2$Ni.

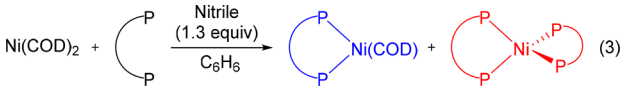

Crystallography: (Phosphine)$_2$Ni Complexes. Single crystals of (dppbenz)$_2$Ni (**10**), (dppmb)$_2$Ni (**11**), (dppb)$_2$Ni (**12**), and a disordered crystal of (DPEPhos)$_2$Ni (**13**) were analyzed. The solid state structures of (dppe)$_2$Ni[12] (**14**) and (dppp)$_2$Ni[13] (**15**) have been previously determined. These data allowed comparisons between the structural properties of (phosphine)$_2$Ni complexes with ligands that differed by the amount of carbons in the aliphatic backbone (such as DPPE, DPPP, and DPPB) and by the rigidity of the backbone (such as DPPB and DPPMB). ORTEP diagrams of complexes **10**–**13** are shown in Figure 2. The average Ni–P bond lengths and average P–Ni–P bond angles of complexes **10**–**12**, **14**, and **15** are shown in Table 4.

Table 4. Average Bond Lengths and Ligand Bite Angles for Complexes 10–12, 14, and 15[a]

entry	complex	average Ni–P bond length	ligand bite angle
1	(dppbenz)$_2$Ni (**10**)	2.157(2) Å	90.6(3)°
2	(dppmb)$_2$Ni (**11**)	2.185(3) Å	106.7°
3	(dppb)$_2$Ni (**12**)	2.2031(6) Å	104.7°
4	(dppe)$_2$Ni (**14**)	2.164(5) Å[12]	90.5(3)°[12]
5	(dppp)$_2$Ni (**15**)	2.177(1) Å[13]	99.52°[13]

[a]Complex **13** not included due to disorder.

These five complexes are all pseudotetrahedral about the Ni. The measured bite angle of DPPE in complex **14** is 90.5(3)°. The bite angle of DPPP in **15** increases to 99.52°. In complex **12**, the bite angle of DPPB is 104.7°. The Ni–P bond lengths also increased as more carbons were added to the backbone of the phosphine ligand. The average bond length for complex **14** was 2.164(5) Å, followed by 2.177(1) Å in **15** and 2.2031(6) Å in **12**.

Next, the (phosphine)$_2$Ni complexes that had ligands varying by the rigidity of their backbones were compared. The first pair of (phosphine)$_2$Ni complexes were (dppe)$_2$Ni (**14**) and (dppbenz)$_2$Ni (**10**). The average Ni–P bond length in **10** was about ∼0.01 Å shorter than the average bond length for **14**. The bite angles of the ligands in each complex were very similar: 90.6(3)° for **10** and 90.5(3)° for **14**.

We compared the crystal structures of (dppb)$_2$Ni (**12**) and (dppmb)$_2$Ni (**11**). DPPB and DPPMB both form seven-membered rings when bound to Ni. The bite angle of DPPB in **12** is 104.7°. In complex **11**, the bite angle of DPPMB is 106.7°. The average Ni–P bond lengths are ∼0.018 Å shorter in **11** as compared to **12**.

Although the single crystal for complex **13** was disordered, two bonds to one ligand were significantly shorter than the two bonds to the opposite ligand. This difference was not observed in any of the other (phosphine)$_2$Ni complexes, where all of the Ni–P bond lengths were nearly identical.

Crystallography: (Phosphine)Ni(cod) Complexes. Single crystals of (DPEPhos)Ni(cod) (**6**), (dppb)Ni(cod) (**7**),

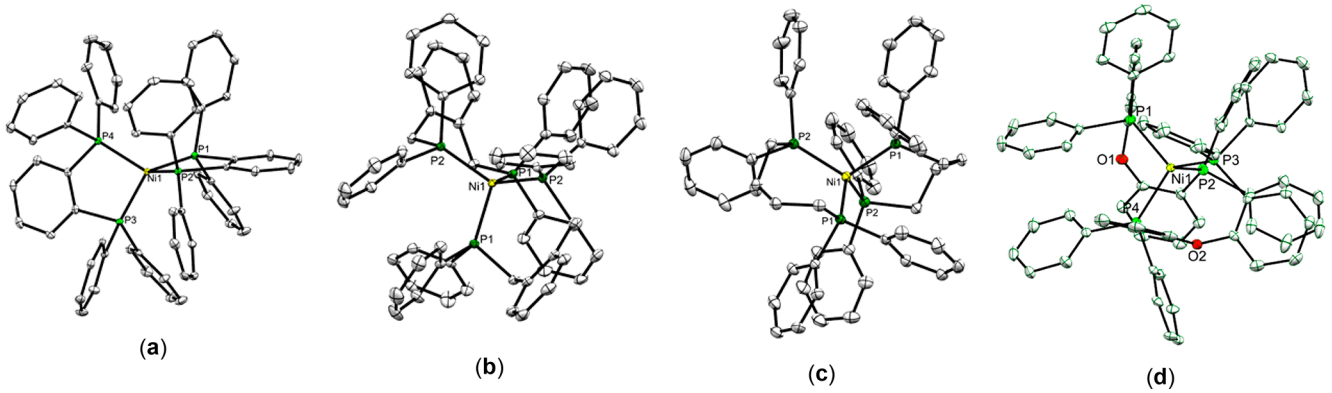

Figure 2. ORTEP diagrams: (dppbenzene)$_2$Ni (**10**) (a), (dppmb)$_2$Ni (**11**) (b), (dppb)$_2$Ni (**12**) (c), and (DPEPhos)$_2$Ni (**13**) (d). Ellipsoids set at 50% probability. Hydrogen atoms omitted for clarity.

DOI: 10.1021/acs.organomet.8b00438
Organometallics XXXX, XXX, XXX–XXX

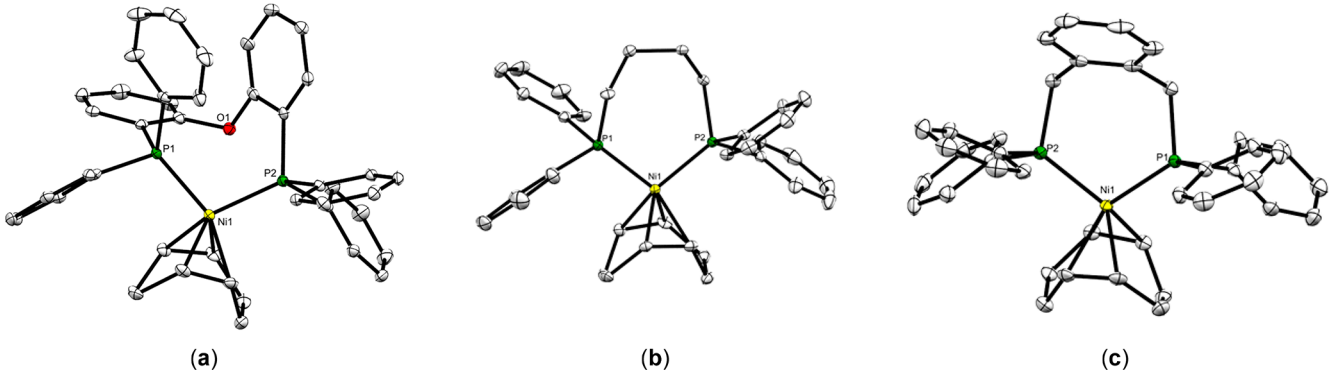

(a) (b) (c)

Figure 3. ORTEP diagrams: (DPEPhos)Ni(cod) (**6**) (a), (dppb)Ni(cod) (**7**) (b), and (dppmb)Ni(cod) (**8**) (c). Ellipsoids set at 50% probability. Hydrogen atoms omitted for clarity.

and (dppmb)Ni(cod) (**8**) (ORTEP diagrams shown in Figure 3) were also studied. Average bond lengths and angles are shown in Table 5. These crystal structures allowed for comparisons between these complexes and also between each of them and their $(phosphine)_2Ni$ counterparts. The first pair of complexes compared were (dppb)Ni(cod) (**7**) and $(dppb)_2Ni$ (**12**). Replacement of one DPPB ligand in **12** with COD, forming **7**, decreases the Ni−P bond length by ∼0.05 Å. The P−Ni−P angle also decreases by ∼2.9°.

Table 5. Average Ni−P Bond Lengths and P−Ni−P Bond Angles for Complexes 6−8

entry	complex	average Ni−P bond length	ligand bite angle
1	(DPEPhos)Ni(cod)(**6**)	2.168(5) Å	105.5°
2	(Dppb)Ni(cod) (**7**)	2.152(1) Å	101.8°
3	(Dppmb)Ni(cod) (**8**)	2.167(1) Å	105.5°

Replacement of one of the DPPMB ligands in **11** with a COD ligand to form **8** decreased the Ni−P bond lengths by ∼0.02 Å. The bite angle of the ligand also decreased by ∼1.2°. These changes are analogous to the changes observed between complexes **7** and **12**.

Finally, complexes **7** and **8** were compared directly (Table 5, entries 2 and 3). The P−Ni−P angle increased by 3.8° in **8** as compared to **7**. The Ni−P bond lengths also increased by ∼0.02 Å.

DISCUSSION

The conclusion previously reached by our group and others that most chelating phosphines form $(phosphine)_2Ni$ complexes when mixed with $Ni(cod)_2$ was confirmed. Attempts to quantify this complex formation and perform comparisons between ligand sets were met with significant challenges. In the beginning of this study, we believed that trends between the different ligands would present themselves. These trends would vary based on the amount of carbons in the backbone of the chelating phosphine, along with the rigidity of the backbone. When we tried to vary the backbones of the ligands using an aliphatic backbone size of one (DPPM), two (DPPE), three (DPPP), four (DPPB), and five (DPPPentane), DPPM and DPPPentane proved to be unsuitable for analysis under the normal conditions due to the formation of multiple side products beyond just (phosphine)Ni(cod) and $(phosphine)_2Ni$, as demonstrated by the observance of multiple resonances in the ^{31}P NMR spectra. These different signals were attributed to conglomerates for DPPM.[14] The large, floppy backbone of DPPPentane means that it is a likely candidate to bind to two Ni centers instead of forming an eight-membered ring with just one Ni center. DPPB hardly formed any $(dppb)_2Ni$ when mixed with $Ni(cod)_2$ (Table 1, column 3, entry 4), while DPPP and DPPE formed significant amounts of $(phosphine)_2Ni$ along with (phosphine)Ni(cod) (Table 1, column 3, entries 1 and 2). This result indicated that the seven-membered ring formed when DPPB binds to Ni is less stable than the six- and five-membered rings formed, respectively, when DPPP and DPPE bind to Ni. In addition, when 15% or 1.3 equiv of benzonitrile was added to the mixture of $Ni(cod)_2$ and DPPB, (dppb)Ni(cod) was observed exclusively while the ratios of (phosphine)Ni(cod)/$(phosphine)_2Ni$ for DPPE and DPPP under the same conditions did not significantly change (Table 1, columns 4−6, entries 1, 2, and 4). The successful isolation of (dppmb)Ni(cod) and (*rac*-binap)Ni(cod) was concurrent with the observation that phosphines forming seven-membered rings with Ni were more susceptible to removal through addition of benzonitrile.

Turning to the literature, a report from 2017 by Sauthier and co-workers found that a system of $Ni(cod)_2$ and either DPPB or DPPMB was efficient at performing hydroalkoxylation of alkenes. DPPE and DPPP were not effective in this reaction, and calculations supported the conclusion that $(dppe)_2Ni$ and $(dppp)_2Ni$ were stable and unlikely to dissociate a phosphine.[15] This conclusion is also supported by literature reports of experiments using chiral phosphines. Kempe and co-workers[16] developed an enantioselective nickel hydrosilyation catalyst system where they utilized $Ni(cod)_2$ and the chiral chelating phosphine DIOP (Figure 4), which has four carbons in the backbone. The active catalyst was suspected to be (diop)Ni(cod) and $(diop)_2Ni$ was isolated and shown to be catalytically inactive. Finally, the report by Hartwig and co-workers mentioned in the introduction uses benzonitrile to eliminate $(binap)_2Ni$ in catalytic reactions. These methods and their results mirror our findings.[6f,h]

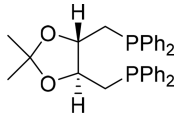

Figure 4. Chiral (*S*,*S*)-DIOP

Trends following the variance of rigidity of the ligand backbones are harder to discern. Four pairs of phosphines were

DOI: 10.1021/acs.organomet.8b00438
Organometallics XXXX, XXX, XXX−XXX

chosen to try and observe trends: DPPE/DPPBenz, DPPB/DPPMB, BIPHEP/BINAP, and DPEPhos/Xantphos. However, each of these pairs had different relationships. DPPE and DPPBenz, being smaller ligands, made (phosphine)$_2$Ni complexes that were not reactive with nitrile. The more rigid DPPBenz formed (dppbenz)Ni(cod) in an 8:1 ratio with (dppbenz)$_2$Ni, while the less rigid DPPE formed (dppe)Ni(cod) in a 1:2 ratio with (dppe)$_2$Ni under the same conditions (Table 1, entries 1 and 7). For DPPB/DPPMB, this relationship was reversed. The less rigid DPPB formed (dppb)Ni(cod) in a 15:1 ratio with (dppb)$_2$Ni (Table 1, column 3, entry 4), while the more rigid DPPMB formed (dppmb)Ni(cod) in a 1:6 ratio with (dppmb)$_2$Ni (Table 1, column 3, entry 8). BIPHEP and BINAP had similar ratios in column 3. (binap)$_2$Ni was reactive with nitrile, while (biphep)$_2$Ni was not. Xantphos and DPEPhos react very differently, despite the only difference being the extra dimethyl connection between the benzene rings on the xanthene backbone. Xantphos forms an insoluble red solid when mixed with Ni(cod)$_2$, which is (Xantphos)$_2$Ni. DPEPhos forms (DPEPhos)Ni(cod) exclusively. A reason for this change in reactivity could be the addition of more steric bulk around the nickel by the less rigid DPEPhos, which can flex and move to ensure more favorable steric and π-stacking[17] interactions with itself rather than with an opposite ligand. Examination of the solid-state structure of complex 13 shows only one π-stacking interaction between the opposite ligands, which may not give enough stabilization to overcome the steric clashes that occur when two DPEPhos ligands bind to Ni.

While we were unable to acquire an ordered solid-state structure of (Xantphos)$_2$Ni, the more rigid nature of the ligand will leave more space around the Ni. This allows for an opposite ligand to bind and gives enough room for favorable π-stacking interactions to occur. Xantphos is also interesting in that (Xantphos)$_2$Ni can be activated for catalysis using benzonitrile.[11] However, experiments using only benzonitrile and COD were largely unsuccessful at forming any (Xantphos)Ni(cod). This illustrates the need for a ligand that binds strongly to Ni (such as an alkyne or strongly backbonding alkene) opposite Xantphos. Other ligands have not shown this effect. DPPB, for example, forms a more stable Ni(0) complex with COD than with a strongly backbonding alkene such as stilbene.

A unique feature was observed with the crystal structure of complex 13. Despite the differing exact bond lengths between different structures in the unit cell and the toluene disorder, the data were clear that one DPEPhos ligand had shorter bond lengths to the Ni than the opposite DPEPhos ligand. As previously stated, DPEPhos only forms (DPEPhos)Ni(cod) when mixed with Ni(cod)$_2$. A possible reason could be that more stability exists in forming shorter Ni−P bonds in (DPEPhos)Ni(cod) rather than forming longer bonds to form (DPEPhos)$_2$Ni. Less steric clashing occurs in complex **6** as compared to that in complex **13**, resulting in the favored formation of complex **6**.

Another correlation observed was that the formation of (phosphine)Ni(cod) was more favorable in a specific range of ligand bite angles. The ligands with bite angles under 100°, such as DPPE, DPPP, and DPPBenz, formed (phosphine)$_2$Ni complexes that were not reactive with benzonitrile. Ligands slightly above this threshold in the range of 102−110° were much more likely to form (phosphine)Ni(cod) or have a (phosphine)$_2$Ni complex that was reactive with benzonitrile. Above a bite angle of 110°, the (phosphine)$_2$Ni complex was reactive with benzonitrile, but the (phosphine)Ni(cod) complex was not as stable as the (phosphine)$_2$complex. The most prominent example was Xantphos (bite angle of 112°).[18] Nitrile can activate (Xantphos)$_2$Ni, but (Xantphos)Ni(cod) was not isolable. While many other factors affect the ligand exchange, the bite angle provides a starting point toward categorizing the ligands. An exception is BINAP. The bite angle of BINAP is 93°, but (binap)$_2$Ni was reactive with nitrile. The steric bulk of the ligand could be destabilizing (binap)$_2$Ni. DPPF also has a bite angle of 96°, and its unique reactivity could be a result of the stereoelectronic properties imparted by the ferrocene backbone.

The variation of the steric and electronic properties of the nitrile also gave key information. With DPPE and DPPP, the use of the electron-withdrawing nitrile did not change the ratio of (phosphine)Ni(cod)/(phosphine)$_2$Ni (Table 3, entry 3). With DPPMB, a significant amount of (dppmb)Ni(η^2-NC(3,5-F)Ph) was observed. Since 3,5-difluorobenzonitrile is electron-deficient, it is much more π-acidic than benzonitrile and thus more suited for nucleophilic attack by the Ni. These results showed that the 3,5-difluorobenzonitrile was causing the removal of a ligand from (dppmb)$_2$Ni in order to form the more stable complex (dppmb)Ni(η^2-NC(3,5-F)Ph).

These studies also showed that the addition of nitrile had very little effect on (dppe)$_2$Ni and (dppp)$_2$Ni because no η^2-NC bound nitrile complex was observed even with 3,5-difluorobenzonitrile. These results further confirm that the distribution of (phosphine)Ni(cod)/(phosphine)$_2$Ni for DPPE and DPPP is governed by the initial reaction of the phosphine with Ni(cod)$_2$. Once (dppe)$_2$Ni and (dppp)$_2$Ni are formed, they are unlikely react with any nitrile to form (phosphine)Ni(cod).

CONCLUSIONS

We have extended our previous research into (Xantphos)Ni(π-L) complexes[11] to inspect the reactions between Ni(cod)$_2$ and many different chelating phosphines beyond Xantphos. The desired precatalyst or active species in reactions utilizing Ni(cod)$_2$ and a chelating phosphine is (phosphine)Ni(cod), and the amount of this complex in a reaction can be increased with the addition of benzonitrile.

The syntheses and full characterizations of more (phosphine)$_2$Ni complexes allowed us to carry out valuable average bond length studies that gave information regarding the relationships between the bond lengths and angles and the propensity of each ligand to form (phosphine)Ni(cod) when reacted with Ni(cod)$_2$. We have previously shown that (Xantphos)$_2$Ni is a moderately air-stable complex that can be activated for catalysis by the addition of benzonitrile.[11] The other (phosphine)$_2$Ni complexes could potentially act the same way.[19]

Our studies suggest the role of nitrile in the displacement of a phosphine from a given (phosphine)$_2$Ni complex (Scheme 1 and Table 3) is quite complex. Experimental and theoretical routes to explore this mechanism are currently underway.

These studies expand the scope of ligands that can be used for Ni(0) catalysis. Complexes **6**−**9** have been isolated and can be used for catalysis with the firm knowledge that no detrimental (phosphine)$_2$Ni or Ni(cod)$_2$ will be present in the reaction. With other ligands, the addition of benzonitrile to the reaction increases the amount of catalytically active (phosphine)Ni(cod). The new knowledge about the extent

DOI: 10.1021/acs.organomet.8b00438
Organometallics XXXX, XXX, XXX−XXX

of active precatalyst will allow for an expansion of the ligand scope in these catalytic reactions and pave the way for new reaction discovery. Efforts are currently underway to use these new complexes and the new knowledge of the effects of adding benzonitrile to these reactions.

EXPERIMENTAL SECTION

General Considerations. All manipulations were carried out in a glovebox under an atmosphere of N_2. All glassware was dried in an oven overnight. Benzene, pentane, and THF were sparged with nitrogen, dried over neutral alumina, and deoxygenated over Q5 under N_2 using a Grubbs type purification system. DPPM, DPPE, DPPP, DPPB, DPPPentane, DPPMB, *rac*-BINAP, DPEPhos, BIPHEP, DPPBenz, DPPF, and Xantphos, were purchased from commercial sources and used as received. Ni(cod)$_2$ was purchased from Strem Chemicals or prepared according to the literature procedure.[20] Deuterated benzene (Cambridge Isotope Laboratories), deuterated THF (Cambridge Isotope Laboratories), and 1,5-cyclooctadiene (COD) were distilled from CaH_2 and degassed using three freeze−pump−thaw cycles. Screw-cap NMR tubes were used for all NMRs. The tubes were cleaned by rinsing with acetone, sonicating with 1:1 THF/concentrated HCl for 1 h, and rinsing again with acetone. NMR spectra were recorded on Varian spectrometers. ^{1}H experiments were recorded at 500 MHz. ^{13}C experiments were recorded at 125 MHz. ^{31}P experiments were recorded at 121 MHz. ^{31}P NMR spectra were referenced to external 85% H_3PO_4 (0 ppm). ^{13}C and ^{31}P experiments were proton-decoupled. ^{1}H and ^{13}C NMRs were referenced to the residual solvent peak for either benzene-d_6 (δ 7.13 and δ 128.6, respectively) or THF-d_8 (δ 3.76 and δ 68.0, respectively). IR spectra were recorded on a Bruker Tensor 27 FT-IR spectrometer. Elemental analyses were performed by Midwest Microlab LLC. The discussed ORTEP diagrams of complexes **6**−**8** and **10**−**13** were created using Mercury.[21]

X-ray Structure. Single crystal X-ray crystallography data were collected and analyzed by Dr. Arnold L. Rheingold at the University of California, San Diego and by Dr. Ryan T. Vanderlinden at the University of Utah.

University of California, San Diego (A.L.R.). The diffraction data were collected on a Bruker Ultra mini rotating anode (Mo) with an Apexil detector and microfocusing optics. The OLEX2[22] software suite was used to manage the data. All data were collected at 100 K. PLATON SQUEEZE[23] was used to account for severely disordered solvent molecules that are not represented in the structure.

University of Utah (R.T.V.). The diffraction data were collected on a Nonius KappaCCD diffractometer equipped with Mo KR radiation (λ = 0.71073 Å) and a BRUKER APEXII CCD detector. The APEX3[24] software suite was used to manage data collection, integration, scaling, absorption correction by the multiscan method (SADABS),[25] structure determination via direct methods (SHLEXT),[26] and model refinement (SHELXL).[27] All data were collected at 103(2) K.

General Procedure for Reactions of Ni(cod)$_2$ and a Phosphine in a 1:1 Ratio (Table 1, Column 3). The phosphine ligand and Ni(cod)$_2$ were mixed in a 1:1 ratio in 0.75 mL of benzene-d_6. The solution was analyzed by ^{31}P and ^{1}H NMR after 2 h and the following day.

General Procedure for Reactions of Ni(cod)$_2$, Phosphine, and Benzonitrile (Table 1, Columns 4−6). The phosphine and Ni(cod)$_2$ were mixed in a 1:1 ratio in benzene, followed by addition of benzonitrile (15%, 1.3 equiv, or 4 equiv) after 30 s. The solutions were analyzed by ^{31}P NMR after 2 h and the following day.

General Procedure for Reactions of Ni(cod)$_2$, Phosphine, Benzonitrile, and Excess COD (Table 1, Columns 7−9). The phosphine and Ni(cod)$_2$ were mixed in a 1:1 ratio in benzene, followed by addition of COD (2, 10, or 20 equiv) after 30 s and addition of benzonitrile (1.3 equiv) after another 30 s. The solutions were analyzed by ^{31}P NMR after 2 h and the following day.

General Procedure for Reactions of Ni(cod)$_2$, Phosphine, and Various Nitriles (Table 3). The phosphine and Ni(cod)$_2$ were mixed in a 1:1 ratio in benzene, followed by addition of a nitrile (1.3 equiv) after 30 s. The solutions were analyzed by ^{31}P NMR after 2 h and the following day.

*(DPEPhos)Ni(cod) (**6**).* DPEPhos (300.2 mg, 0.557 mmol) and Ni(cod)$_2$ (153.3 mg, 0.557 mmol) were added to a 20 mL scintillation vial equipped with a stir bar. Benzene (2 mL) was added, and the solution was stirred for 12 h. Pentane (15 mL) was then added, and the vial was stored at −38 °C overnight. Subsequent filtration gave an orange solid which was complex **6** (334.5 mg, 473.5 mmol, 85%). Crystals suitable for X-ray diffraction were grown from the layering of 1 mL of pentane over a saturated solution of the complex in 0.5 mL of benzene. ^{1}H NMR (500 MHz, C_6D_6): δ 7.57 (t, J = 5 Hz, 8H), 7.11 (t, J = 5 Hz, 2H), 7.00 (m, 12H), 6.74 (m, 4H), 6.52 (t, J = 5 Hz, 2H), 4.61 (d, J = 5 Hz, 4H, vinylic COD), 1.86 (t, J = 10 Hz, 4H, aliphatic COD), 1.76 (s, 4H). ^{13}C{^{1}H} NMR (125 MHz, C_6D_6): δ 160.5 (d, J = 12.5 Hz), 137.6 (dd, J = 25, 5 Hz), 133.7 (d, J = 12.5 Hz), 133.7 (s), 129.5 (s), 123.2 (d, J = 1.25 Hz), 121.7 (t, J = 2.5 Hz), 84.7 (d, J = 6.25 Hz), 29.7 (d, J = 3.75 Hz). ^{31}P{^{1}H} NMR (C_6D_6): δ 33.1 (s). IR (nujol, NaCl): δ 3071 (m), 3048 (m), 2872 (m), 2726 (m), 2669 (w), 1959 (w), 1653 (m), 1586 (s), 1562 (m), 1309 (w), 1259 (m), 1204 (w), 1095 (w), 1069 (m), 743 (w), 772 (m), 525 (m). Anal. Calcd for $C_{44}H_{40}NiP_2O$: C,74.96; H, 5.71. Found: C, 74.68; H, 5.73.

*(dppb)Ni(cod) (**7**).* DPPB (77.5 mg, 0.182 mmol) and Ni(cod)$_2$ (50 mg, 0.182 mmol) were added to a 20 mL scintillation vial equipped with a stir bar. Benzene (1 mL) was added, and the reaction was stirred for 5 min. COD (288 μL, 2.35 mmol) was added, followed by benzonitrile (24.3 μL, 0.236 mmol). The heterogeneous yellow solution was stirred overnight. Pentane (15 mL) was added, and the vial was stored overnight at −38 °C. The solution was then filtered through a medium frit, yielding 7 as a bright yellow solid (102.1 mg, 0.172 mmol, 95%). Yellow crystals suitable for X-ray diffraction were grown by layering 1 mL of pentane on to a saturated solution of the complex in 0.5 mL of benzene. ^{1}H NMR (500 MHz, C_6D_6): δ 7.46 (t, J = 10 Hz, 8H), 7.15 (t, J = 10 Hz, 8H), 7.08 (t, J = 10 Hz, 4H), 4.39 (d, J = 10 Hz, 4H), 2.16 (s, 4H), 1.84 (t, J = 10 Hz, 4H), 1.58 (s, 4H), 1.17 (s, 2H), 1.13 (s, 2H). ^{13}C{^{1}H} NMR (125 MHz, C_6D_6) δ 141.2 (d, J = 30 Hz), 132.4 (t, 6.25 Hz), 83.5 (t, 2.5 Hz), 67.4 (s), 35.2 (m), 29.8 (s), 25.4 (s) 24.8 (s). ^{31}P{^{1}H} NMR (121 MHz, C_6D_6): δ 35.9 (s). IR (nujol, NaCl, cm^{-1}): 3071 (m), 3050 (m), 3018 (s), 2029 (w), 1959 (m), 1585 (w), 1537 (s), 1377 (m), 1323 (w), 1300 (m), 1180 (m), 1155 (m), 1098 (w), 1025 (w), 719 (br), 623 (w). Anal. Calcd for $C_{36}H_{40}NiP_2$: C. 72.87; H, 6.79. Found: C, 72.45; H, 6.81.

*(dppmb)Ni(cod) (**8**).* DPPMB (258 mg, 0.543 mmol) and Ni(cod)$_2$ (149 mg, 0.543 mmol) were added to a 20 mL scintillation vial equipped with a stir bar. THF (10 mL) was added, and the reaction was stirred for 5 min. COD (4.2 mL, 34.3 mmol) was added, followed by benzonitrile (76 μL, 0.591 mmol). The homogeneous yellow solution was then stirred for 4 days. The volatiles were removed under vacuum. Pentane (15 mL) was added, and the vial was stored overnight at −38 °C. The solution was filtered through a medium frit, yielding **8** as a bright yellow solid (299.4 mg, 0.466 mmol, 86%). Crystals suitable for X-ray diffraction were grown by layering 1 mL of pentane on to a saturated solution of the complex in 0.5 mL of benzene. ^{1}H NMR (C_6D_6): δ 7.56 (t, J = 10 Hz, 8H), 7.15 (t, J = 10 Hz, 12H), 6.44 (m, 2H), 6.11 (m, 2H), 4.41 (d, J = 10 Hz, 4H), 3.65 (d, J = 5 Hz, 4H), 1.86−1.64 (m, 8H). ^{13}C{^{1}H} NMR (C_6D_6) δ 139.8 (dd, J = 22.5, 3.75), 134.2 (s) 132.0 (d, 30 Hz), 132.0 (s), 129.5 (t, 5 Hz), 127.5 (s) 124.0 (s) 84.9 (t, 6.25 Hz), 84.9 (d, 6.25 Hz), 39.8 (d, 14 Hz), 33.1 (s), 29.1 (t, 2.5 Hz), 27.1 (s), 21.4 (s), 13.0 (s). ^{31}P{^{1}H} NMR (C_6D_6) δ 27.4 (s). Anal. Calcd for $C_{40}H_{40}NiP_2$: C. 74.90 H. 6.28. Found: C. 74.63 H. 5.97.

*(rac-binap)Ni(cod) (**9**).* BINAP (72.1 mg, 0.115 mmol) and Ni(cod)$_2$ (31.8 mg, 0.115 mmol) were weighed into a 20 mL scintillation vial. Benzene (3 mL) was added, followed by benzonitrile (15.4 μL, 0.149 mmol) and COD (141 μL, 1.15 mmol). The solution went from yellow to gray to black, and was stirred for 18 h, after which the volatiles were removed. Pentane (15 mL) was added, and the vial was stored overnight at −38 °C. Subsequent filtration through a medium frit yielded **9** as a brown/black solid (61.6 mg, 0.078 mmol,

DOI: 10.1021/acs.organomet.8b00438
Organometallics XXXX, XXX, XXX−XXX

67%). ^{1}H NMR (500 MHz, THF-d_8): δ 8.28 (t, J = 10 Hz, 2H), 7.96 (t, J = 10 Hz, 4H), 7.77 (d, J = 10 Hz, 2H), 7.60 (m, 8H), 7.24 (t, J = 10 Hz, 2H), 7.11 (m, 4H), 6.83 (t, J = 10 Hz, 2H), 6.59 (s, 6H), 4.75 (s, 2H, vinylic COD), 4.53 (s, 2H, vinylic COD), 1.96 (s, 2H, under solvent peak, aliphatic COD), 1.90 (s, 2H, under solvent peak, aliphatic COD), 1.74 (s, 2H, aliphatic COD), 1.55 (s, 2H, aliphatic COD). ^{13}C NMR (125 MHz, THF-d_8): δ 140.0 (s), 139.7 (s), 138.6 (s), 138.4 (s), 138.1 (s), 137.9 (s), 135.4 (d, J = 12.5 Hz), 135.1 (d, J = 12.5 Hz), 134.9 (s), 134.0 (s), 128.7 (s), 128.5 (d, J = 12.5 Hz), 128.2 (s), 128.1 (s), 126.7 (s), 126.6 (s), 126.4 (s), 126.2 (s), 86.1 (s), 83.8 (s), 30.4 (s), 30.1 (s), 29.4 (s). ^{31}P NMR (121 MHz, THF-d_8): δ 33.6 (s). IR (nujol, NaCl, cm^{-1}): 3168 (w), 3142 (m), 3052 (s), 2726 (m), 2668 (m), 1585 (w), 1303 (m), 1156 (m), 1088 (w), 1027 (m), 965 (m), 890 (w), 722 (m), 696 (w), 673 (w), 524 (w). Anal. Calcd for $C_{52}H_{44}NiP_2$: C, 79.10; H, 5.62. Found: C, 78.74; H, 5.76.

*(dppbenz)$_2$Ni (**10**).* DPPBenz (143.4 mg, 0.321 mmol) and Ni(cod)$_2$ (44.2 mg, 0.161 mmol) were weighed into a 5 mL vial. Benzene (1 mL) was added, and the solution was stirred for 24 h. Pentane (4 mL) was then added to the orange heterogeneous solution. The reaction was stored at −40 °C overnight. The liquid was removed using a pipet, and the orange solid was washed 2 times with 5 mL of pentane and then dried under high vacuum. Complex **10** was recovered as an orange solid (150.3 mg, 0.158 mmol, 98%). Orange crystals suitable for X-ray diffraction analysis were grown by dissolving a small-scale version of the reaction in benzene and letting the solution sit undisturbed for 24 h. ^{1}H NMR (500 MHz, THF-d_8): δ 7.48 (s, 4H), 7.43 (s, 20H), 7.18 (t, J = 10 Hz, 8H), 7.03 (t, J = 10 Hz, 16H), ^{13}C{^{1}H} NMR (125 MHz, THF-d_8): δ 150.7 (m), 140.2 (m), 133.5 (t, J = 6.25 Hz), 129.6 (s), 129.5 (s), 128.8 (s), 128.2 (s). ^{31}P{^{1}H} NMR (121 MHz, C_6D_6): 48.02 (s). Anal. Calcd for $C_{60}H_{48}NiP_4$: C, 75.73; H, 5.08. Found: C, 75.56; H, 5.15.

*(dppb)$_2$Ni (**12**).* DPPB (153.8 mg, 0.369 mmol) and Ni(cod)$_2$ (50.8 mg, 0.185 mmol) were weighed into a 20 mL scintillation vial. Benzene (1 mL) was added, and the solution was stirred for 24 h. Pentane (4 mL) was then added to the heterogeneous yellow solution. The reaction was stored at −40 °C overnight. The liquid was removed using a pipet, and the solid was washed 2 times with 5 mL of pentane and then dried under high vacuum. Complex **12** was recovered as a yellow solid (150.4 mg, 0.169 mmol, 91%). Yellow crystals suitable for X-ray diffraction analysis were grown by dissolving a small-scale version of the reaction in benzene and letting the solution sit undisturbed for 24 h. ^{1}H NMR (500 MHz, C_6D_6): δ 7.55 (s, 16H), 7.01 (m, 24H), 2.03 (s, 8H), 1.24 (s, 8H). ^{13}C{^{1}H} NMR (125 MHz, C_6D_6): δ 134.1 (s), 128.9 (s), 128.7 (s), 128.5 (s), 128.2 (s), 128.1 (s), 31.7 (q, J = 7.5 Hz), 24.5 (s). ^{31}P{^{1}H} NMR (121 MHz, C_6D_6): δ 19.36 (s). Anal. Calcd for $C_{56}H_{56}NiP_4$: C, 73.78; H, 6.19. Found: C, 73.52; H, 6.26.

■ ASSOCIATED CONTENT

Supporting Information

The Supporting Information is available free of charge on the ACS Publications website at DOI: 10.1021/acs.organomet.8b00438.

NMR spectra and crystallographic data (PDF)
Cartesian coordinates (XYZ)

Accession Codes

CCDC 1850155−1850160 and 1850175 contain the supplementary crystallographic data for this paper. These data can be obtained free of charge via www.ccdc.cam.ac.uk/data_request/cif, or by emailing data_request@ccdc.cam.ac.uk, or by contacting The Cambridge Crystallographic Data Centre, 12 Union Road, Cambridge CB2 1EZ, UK; fax: +44 1223 336033.

■ AUTHOR INFORMATION

Corresponding Author

*E-mail: louie@chem.utah.edu.

ORCID

Nicholas D. Staudaher: 0000-0002-5720-0949
Janis Louie: 0000-0003-3569-1967

Notes

The authors declare no competing financial interest.

■ ACKNOWLEDGMENTS

We gratefully acknowledge the National Institute of Health (GM076125) for financial support. We also thank Mia Yu for assistance in final synthesis and characterization of the new complexes.

■ REFERENCES

(1) Biffis, A.; Centomo, P.; Del Zotto, A.; Zecca, M. Pd Metal Catalysts for Cross-Couplings and Related Reactions in the 21st Century: A Critical Review. *Chem. Rev. (Washington, DC, U. S.)* **2018**, *118*, 2249−2295.

(2) Matsui, J. K.; Lang, S. B.; Heitz, D. R.; Molander, G. A. Photoredox-Mediated Routes to Radicals: The Value of Catalytic Radical Generation in Synthetic Methods Development. *ACS Catal.* **2017**, *7*, 2563−2575.

(3) Noverges Pedro, B.; Medio-Simon, M.; Jutand, A. Influence of the Ligand of Palladium(0) Complexes on the Rate of the Oxidative Addition of Aryl and Activated Alkyl Bromides: Csp^2-Br versus Csp^3-Br Reactivity and Selectivity. *ChemCatChem* **2017**, *9*, 2136−2144.

(4) (a) Dander, J. E.; Garg, N. K. Breaking Amides using Nickel Catalysis. *ACS Catal.* **2017**, *7*, 1413−1423. (b) Standley, E. A.; Tasker, S. Z.; Jensen, K. L.; Jamison, T. F. Nickel Catalysis: Synergy between Method Development and Total Synthesis. *Acc. Chem. Res.* **2015**, *48*, 1503−1514. (c) Tasker, S. Z.; Standley, E. A.; Jamison, T. F. Recent advances in homogeneous nickel catalysis. *Nature (London, U. K.)* **2014**, *509*, 299−309. (d) Tobisu, M.; Chatani, N. Cross-Couplings Using Aryl Ethers via C-O Bond Activation Enabled by Nickel Catalysts. *Acc. Chem. Res.* **2015**, *48*, 1717−1726. (e) Chierchia, M.; Law, C.; Morken, J. P. Nickel-Catalyzed Enantioselective Conjunctive Cross-Coupling of 9-BBN Borates. *Angew. Chem., Int. Ed.* **2017**, *56*, 11870−11874. (f) Iwasaki, T.; Kambe, N. Ni-Catalyzed C-C Couplings Using Alkyl Electrophiles. *Top. Curr. Chem.* **2017**, *374*, 1−36. (g) Joe, C. L.; Doyle, A. G. Direct Acylation of C(sp3)-H Bonds Enabled by Nickel and Photoredox Catalysis. *Angew. Chem., Int. Ed.* **2016**, *55*, 4040−4043. (h) Mesganaw, T.; Garg, N. K. Ni- and Fe-Catalyzed Cross-Coupling Reactions of Phenol Derivatives. *Org. Process Res. Dev.* **2013**, *17*, 29−39. (i) Tassone, J. P.; MacQueen, P. M.; Lavoie, C. M.; Ferguson, M. J.; McDonald, R.; Stradiotto, M. Nickel-Catalyzed N-Arylation of Cyclopropylamine and Related Ammonium Salts with (Hetero)aryl (Pseudo)halides at Room Temperature. *ACS Catal.* **2017**, *7*, 6048−6059. (j) Wang, J.; Meng, G.; Xie, K.; Li, L.; Sun, H.; Huang, Z. Mild and Efficient Ni-Catalyzed Biaryl Synthesis with Polyfluoroaryl Magnesium Species: Verification of the Arrest State, Uncovering the Hidden Competitive Second Transmetalation and Ligand-Accelerated Highly Selective Monoarylation. *ACS Catal.* **2017**, *7*, 7421−7430.

(5) Wu, K.; Doyle, A. G. Parameterization of phosphine ligands demonstrates enhancement of nickel catalysis via remote steric effects. *Nat. Chem.* **2017**, *9*, 779−784.

(6) (a) Clark, J. S. K.; Voth, C. N.; Ferguson, M. J.; Stradiotto, M. Evaluating 1,1′-Bis(phosphino)ferrocene Ancillary Ligand Variants in the Nickel-Catalyzed C-N Cross-Coupling of (Hetero)aryl Chlorides. *Organometallics* **2017**, *36*, 679−686. (b) Cao, X.; Sha, S.-C.; Li, M.; Kim, B.-S.; Morgan, C.; Huang, R.; Yang, X.; Walsh, P. J. Nickel-catalyzed arylation of heteroaryl-containing diarylmethanes: exceptional reactivity of the Ni(NIXANTPHOS)-based catalyst. *Chem. Sci.* **2016**, *7*, 611−618. (c) Tobisu, M.; Takahira, T.; Morioka, T.; Chatani, N. Nickel-Catalyzed Alkylative Cross-Coupling of Anisoles with Grignard Reagents via C-O Bond Activation. *J. Am. Chem. Soc.* **2016**, *138*, 6711−6714. (d) Xiao, J.; Yang, J.; Chen, T.; Han, L.-B. Nickel-Catalyzed α-Benzylation of Arylacetonitriles via C-O Activa-

DOI: 10.1021/acs.organomet.8b00438
Organometallics XXXX, XXX, XXX−XXX

tion. *Adv. Synth. Catal.* **2016**, *358*, 816−819. (e) Dawson, D. D.; Jarvo, E. R. Stereospecific Nickel-Catalyzed Cross-Coupling Reactions of Benzylic Ethers with Isotopically-Labeled Grignard Reagents. *Org. Process Res. Dev.* **2015**, *19*, 1356−1359. (f) Ge, S.; Green, R. A.; Hartwig, J. F. Controlling First-Row Catalysts: Amination of Aryl and Heteroaryl Chlorides and Bromides with Primary Aliphatic Amines Catalyzed by a BINAP-Ligated Single-Component Ni(0) Complex. *J. Am. Chem. Soc.* **2014**, *136*, 1617−1627. (g) Tollefson, E. J.; Dawson, D. D.; Osborne, C. A.; Jarvo, E. R. Stereospecific Cross-Coupling Reactions of Aryl-Substituted Tetrahydrofurans, Tetrahydropyrans, and Lactones. *J. Am. Chem. Soc.* **2014**, *136*, 14951−14958. (h) Ge, S.; Hartwig, J. F. Nickel-Catalyzed Asymmetric α-Arylation and Heteroarylation of Ketones with Chloroarenes: Effect of Halide on Selectivity, Oxidation State, and Room-Temperature Reactions. *J. Am. Chem. Soc.* **2011**, *133*, 16330−16333. (i) Kumar, P.; Prescher, S.; Louie, J. A Serendipitous Discovery: Nickel Catalyst for the Cycloaddition of Diynes with Unactivated Nitriles. *Angew. Chem., Int. Ed.* **2011**, *50*, 10694−10698. (j) Kumar, P.; Troast, D. M.; Cella, R.; Louie, J. Ni-Catalyzed Ketene Cycloaddition: A System That Resists the Formation of Decarbonylation Side Products. *J. Am. Chem. Soc.* **2011**, *133*, 7719−7721.

(7) Chen, M.-T.; Lee, W.-Y.; Tsai, T.-L.; Liang, L.-C. Nickel(II) complexes containing bidentate diarylamido phosphine chelates: Kumada couplings kinetically preferred to β-hydrogen elimination. *Organometallics* **2014**, *33*, 5852−5862.

(8) (a) Cai, M.-Z.; Jiang, M.-H.; Li, H.-G. A facile stereoselective synthesis of (E)-1-arylseleno-2-aryl-sulfanylethenes via hydrozirconation of arylselenoethynes. *J. Chem. Res.* **2006**, *2006*, 702−704. (b) Wu, Y.; Liu, L.; Yan, K.; Xu, P.; Gao, Y.; Zhao, Y. Nickel-catalyzed decarboxylative C-P cross-coupling of alkenyl acids with P(O)H compounds. *J. Org. Chem.* **2014**, *79*, 8118−8127.

(9) (a) Duerr, A. B.; Yin, G.; Kalvet, I.; Napoly, F.; Schoenebeck, F. Nickel-catalyzed trifluoromethylthiolation of Csp^2-O bonds. *Chem. Sci.* **2016**, *7*, 1076−1081. (b) Yin, G.; Kalvet, I.; Englert, U.; Schoenebeck, F. Fundamental Studies and Development of Nickel-Catalyzed Trifluoromethylthiolation of Aryl Chlorides: Active Catalytic Species and Key Roles of Ligand and Traceless MeCN Additive Revealed. *J. Am. Chem. Soc.* **2015**, *137*, 4164−4172. (c) Lejkowski, M. L.; Lindner, R.; Kageyama, T.; Bodizs, G. E.; Plessow, P. N.; Mueller, I. B.; Schaefer, A.; Rominger, F.; Hofmann, P.; Futter, C.; Schunk, S. A.; Limbach, M. The First Catalytic Synthesis of an Acrylate from CO_2 and an Alkene-A Rational Approach. *Chem. - Eur. J.* **2012**, *18*, 14017−14025. (d) Mori, M.; Kimura, M.; Takahashi, Y.; Tamaru, Y. Nickel catalyzed Grob fragmentation: ω-dienyl aldehydes synthesis. *Chem. Commun. (Cambridge, U. K.)* **2006**, 4303−4305. (e) Kranenburg, M.; Kamer, P. C. J.; van Leeuwen, P. W. N. M.; Vogt, D.; Keim, W. Effect of the bite angle of diphosphine ligands on activity and selectivity in the nickel-catalyzed hydrocyanation of styrene. *J. Chem. Soc., Chem. Commun.* **1995**, 2177−2178. (f) Tsuda, T.; Hasegawa, N.; Saegusa, T. Nickel(0)-catalyzed novel cooligomerization of ethoxy-(trimethylsilyl)ethyne with carbon dioxide to 4,6-diethoxy-3-[1-ethoxy-2,2-bis(trimethylsilyl)vinyl]-5-(trimethylsilyl)-2-pyrone. *J. Chem. Soc., Chem. Commun.* **1990**, 945−947.

(10) Staudaher, N. D.; Arif, A. M.; Louie, J. Synergy between experimental and computational chemistry reveals the mechanism of decomposition of nickel-ketene complexes. *J. Am. Chem. Soc.* **2016**, *138*, 14083−14091.

(11) Staudaher, N. D.; Stolley, R. M.; Louie, J. Synthesis, mechanism of formation, and catalytic activity of Xantphos nickel π-complexes. *Chem. Commun. (Cambridge, U. K.)* **2014**, *50*, 15577−15580.

(12) Hartung, H.; Baumeister, U.; Walther, B.; Maschmeier, M. Crystal and molecular structure of bis[1,2-bis(diphenylphosphino)-ethane]nickel(0). *Z. Anorg. Allg. Chem.* **1989**, *578*, 177−184.

(13) Davies, S. C.; Duff, S. E.; Evans, D. J. Bis[1,3-bis-(diphenylphosphino)propane-κ^2P,P']nickel(0). *Acta Crystallogr., Sect. E: Struct. Rep. Online* **2005**, *61*, m571−m573.

(14) (a) Li, J.; Hor, T. S. A. Formation of $[PtPd_2(\mu^3\text{-}X)_2(P\text{-}P)(dppmX)_2]^{2+}$ (X = S, Se; P-P = dppe, 2 × PPh_3) aggregates through activation of the chalcogen-rich $[PtX_4]$ ring by a PdI-PdI bond. *Dalton Trans* **2008**, 5708−5711. (b) Szlyk, E.; Szymanska, I.; Surdykowski, A.; Glowiak, T.; Wojtczak, A.; Golinski, A. X-Ray crystal structure of $[Ag_4(\mu\text{-dppm})_2(\mu\text{-}C_2F_5COO)_4]$. Synthesis and spectroscopy of silver(I) perfluorinated carboxylate complexes with bis-(diphenylphosphino)methane. *Dalton Trans* **2003**, 3404−3410.

(15) Mifleur, A.; Merel, D. S.; Mortreux, A.; Suisse, I.; Capet, F.; Trivelli, X.; Sauthier, M.; Macgregor, S. A. Deciphering the Mechanism of the Nickel-Catalyzed Hydroalkoxylation Reaction: A Combined Experimental and Computational Study. *ACS Catal.* **2017**, *7*, 6915−6923.

(16) Irrgang, T.; Schareina, T.; Kempe, R. The development of an enantioselective nickel hydrosilylation catalyst system via multi-substrate screening. *J. Mol. Catal. A: Chem.* **2006**, *257*, 48−52.

(17) (a) Sinnokrot, M. O.; Sherrill, C. D. Highly Accurate Coupled Cluster Potential Energy Curves for the Benzene Dimer: Sandwich, T-Shaped, and Parallel-Displaced Configurations. *J. Phys. Chem. A* **2004**, *108*, 10200−10207. Sinnokrot, M. O.; Valeev, E. F.; Sherrill, C. D. Estimates of the Ab Initio Limit for π-π Interactions: The Benzene Dimer. *J. Am. Chem. Soc.* **2002**, *124*, 10887−10893.

(18) Dierkes, P.; van Leeuwen, P. W. N. M. The bite angle makes the difference: a practical ligand parameter for diphosphine ligands. *J. Chem. Soc., Dalton Trans.* **1999**, 1519−1530.

(19) Bricout, H.; Carpentier, J.-F.; Mortreux, A. Nickel-catalyzed substitution reactions of allylic compounds with soft nucleophiles: an efficient alternative to palladium catalysis. *J. Chem. Soc., Chem. Commun.* **1995**, 1863−1864.

(20) Montgomery, J. Product class 1: organometallic complexes of nickel. *Sci. Synth.* **2002**, *1*, 11−62.

(21) Macrae, C. F.; Bruno, I. J.; Chisholm, J. A.; Edgington, P. R.; McCabe, P.; Pidcock, E.; Rodriguez-Monge, L.; Taylor, R.; van de Streek, J.; Wood, P. A. Mercury CSD 2.0 - new features for the visualization and investigation of crystal structures. *J. Appl. Crystallogr.* **2008**, *41*, 466−470.

(22) Dolomanov, O. V.; Bourhis, L. J.; Gildea, R. J.; Howard, J. A. K.; Puschmann, H. OLEX2: a complete structure solution, refinement and analysis program. *J. Appl. Crystallogr.* **2009**, *42*, 339−341.

(23) Spek, A. L. PLATON SQUEEZE: a tool for the calculation of the disordered solvent contribution to the calculated structure factors. *Acta Crystallogr., Sect. C: Struct. Chem.* **2015**, *71*, 9−18.

(24) *APEX3*, 2017−3−0; Bruker AXS Inc.: Madison, WI, 2017.

(25) Krause, L.; Herbst-Irmer, R.; Sheldrick, G. M.; Stalke, D. Comparison of silver and molybdenum microfocus X-ray sources for single-crystal structure determination. *J. Appl. Crystallogr.* **2015**, *48*, 3−10.

(26) Sheldrick, G. M. SHELXT - Integrated space-group and crystal-structure determination. *Acta Crystallogr., Sect. A: Found. Adv.* **2015**, *71*, 3−8.

(27) Sheldrick, G. M. Crystal structure refinement with SHELXL. *Acta Crystallogr., Sect. C: Struct. Chem.* **2015**, *71*, 3−8.

DOI: 10.1021/acs.organomet.8b00438
Organometallics XXXX, XXX, XXX−XXX